

Design and Analysis of the Impact of Ultraviolet Aging on the Mechanical Properties and Durability of PLA Lattice Structures

Abstract

This study explores the design and performance evaluation of PLA (Polylactic acid) lattice structures, with a focus on understanding the eventuality of UV (Ultraviolet) radiation exposure on their mechanical properties. Utilizing Siemens NX software, a 40mm cubic lattice structure with 8mm squared perforations, was designed for optimal performance. With the use of compressive tests, the properties and structural integrity of the 3D printed lattice structures of 50.4% porosity were put to the test. Comprehensive analysis of the stress-displacement data revealed critical insights into the modes of failure as they were aged. Results indicated that short wave UV exposure of wavelength between 365 to 295 nm increased the brittleness of the PLA structures, as evidenced by higher Young's modulus and enhanced compressive strength over time. However, prolonged aging also led to increased displacement on the maximum compressive force from 2.72mm to 3.21mm and compressive strain at the maximum compressive force from 6.81% to 8.02%, suggesting progressive material deterioration. Findings from this study add to a deeper perception of the behavior of PLA under accelerated testing, simulating environmental effects, informing future design and material selection for improved durability and performance in engineering applications. This study provides an understanding of the performance of PLA under UV exposure, contributing to the development of more sustainable additive manufacturing materials, as the findings highlighted the need for careful consideration of the effects UV aging in the design and application of PLA lattice structures.

Keywords: PLA, Lattice structures, Additive manufacturing, Aging test, Sustainable Design

1. Introduction

Additive Manufacturing constructs parts by sequentially layering material from a digital model, enabling the creation of intricate designs that are often unachievable with traditional manufacturing techniques. Techniques such as Fused Deposition Modeling (FDM) are widely used for producing PLA (Polylactic acid) components due to their cost-effectiveness and accessibility. Lattice structures in Additive Manufacturing are used to optimize features such as lightweight design, increased energy absorption, heat transfer, insulation, and material reduction [1]. Lattice structures consist of interlinked permeable unit cells that are organized in a regular and periodic pattern. They provide a suitable environment for cell attachment and colonization in tissue engineering applications [2]. Tao and Leu [3], review that the mechanical characteristics of Lattice Structures can be analysed through experimental tests, numerical simulations, and analytical models. The design of lattice structures with various materials for numerous applications seems limitless, thereby generating the quest for more research and comprehensive reviews. However, reviews on specific applications of lattice structures in fields like tissue engineering have been reported [4].

PLA is an eco-friendly thermoplastic derived from renewable sources such as sugarcane or corn starch. It is popular in Additive Manufacturing due to its ease of printing, good mechanical properties, and environmental benefits. However, PLA's mechanical performance can be influenced by environmental factors, necessitating thorough analysis for applications requiring durability. This reinforcement can be achieved by incorporating bio-derived fibers or nanoparticles into the PLA matrix [5]. PLA composites have been successfully processed into filaments suitable for FDM (Fused deposition modelling) 3D

printing. For example, PLA composites enhanced with regenerated cellulose fibers (lyocell) have been employed in 3D printing, resulting in higher Young's modulus of the filaments [6].

According to Muthe, Pickering and Gauss [5], PLA is extensively used as a filament material in FDM 3D printing because of its low melting point, high tensile strength, minimal thermal expansion, and excellent layer adhesion. However, it should be noted that PLA displays limited heat tolerance unless subjected to annealing. The addition of fillers or nanofillers to PLA composites has been investigated to improve their properties. For example, the addition of carbon black has been shown to influence the properties of plasticized PLA composites [7]. PLA composites reinforced with cellulose fibers and polyethylene glycol (PEG) as an additive have been studied for 3D printing applications. The use of nanocellulose as a filler in PLA composites has shown promise in improving mechanical properties [8].

Factors such as relative density, types of unit cells, and arrangements of cells impact the mechanical characteristics of lattice structures, including stiffness and strength [9]. Different unit cell types, including simple cubic, body-centered cubic, and truncated octahedron, have been studied for lattice structure design [9]. The integration of lattice structures with functionally graded materials has been explored to enhance their performance in applications like orthopedic implants [10]. Design optimization frameworks combining modeling, finite element analysis (FEA), genetic algorithms, and optimization techniques have been proposed to tailor the mechanical behavior of lattice structures [11].

1.1. Literature Review

1.1.1. UV Radiation Exposure

UV exposure can lead to the degradation of composite surfaces and chemical alterations, potentially affecting the overall performance of the material [12]. The alterations in the chemical and physical properties of PLA/TiO₂ nanocomposites over time verify the photocatalytic activity of TiO₂. Exposure to UV radiation can induce chain scission in PLA, resulting in reduced molecular weight and diminished mechanical properties [13]. Studies have shown significant mass loss and molar mass reduction of PLA within a relatively short period of UV exposure, where the oxidative degradation of PLA through UV exposure causes random chain scission, resulting in a reduction of the molar mass [14]. The incorporation of light-responsive nanoparticles or nucleation agents can enhance the photodegradation process [15]. Kalwik *et al.* [16], research paper examines the effects of accelerated UV aging on polymer substances structural properties such as PP30T, PE, and POM. The study employs DSC (Differential Scanning Calorimetry) to evaluate the structure of these materials before and after UV ageing, particularly examining the surface layer where the most significant changes were noted. Kalwik *et al.* [16], states that solar radiation intensity in Europe is approximately 120 kLy per year, with 1.33 W/m² radiation intensity, which is equivalent to 100 hours of laboratory aging tests. At a lower radiation intensity (0.89 W/m²), the total test duration was 600 hours which is equivalent to 4 years of natural aging conditions. The research paper by Wang *et al.* [14], investigates how UV radiation affects the mechanical and physical properties of three-proof polyurethane coatings and polyurethane resins. The study assesses changes in mechanical properties and gloss levels of the materials over time under UV exposure. Techniques such as scanning SEM (Scanning electron microscopy), FTIR (Fourier Transform Infrared spectroscopy), TGA (Thermogravimetric Analysis), and DTG (Differential Thermogravimetry) were employed to analyze the structure of the materials. Wang *et al.* [17], reports that protective coatings' shine deteriorated more than that of individual resins under aging conditions, with significant reductions observed following 1200 hours of exposure to irradiation. Additionally, the tensile strength of resins consistently falls with aging, while the elongation at break initially falls, then rises, and finally falls again after prolonged exposure.

1.1.2. Mechanical Properties

Compressive testing evaluates the lattice structure's ability to withstand loads without deformation or failure. Compression test affects the mechanical characteristics such as strength, modulus and energy absorption [18], also affect the aging time and impact position [19]. Milodinet *al.*[20], studied the mechanical properties of lattice structures produced via additive manufacturing, examining topologies such as diamond, octet, and cubic geometries. They fabricated five specimens with 60% porosity and varied dimensions, considering building orientation and layer thickness; their compressive tests demonstrated similar behavior in the diamond and octet structures, while the cube lattice structure exhibited a distinct response, highlighting the impact of design and manufacturing parameters on mechanical properties. Predicting the compressive strength of composite lattice structures for space launch vehicles, emphasizing the importance of lightweight yet strong structures. Jeon *et al.*[21], introduced a method involving compression tests on sub-element specimens to establish a failure criterion for predicting compressive strength. This technique accounts for the results of bending deformations both in and out of plane of the structure's ribs on compressive strength, aiming for a prediction error margin of 5%. The study found that stress levels varied across different lattice cell geometries, with the Diamond cell exhibiting significantly higher stress values compared to the Dode Thin cell geometry, highlighting structural differences[21]. Compression tests were conducted to evaluate the energy absorption capacity of lattice structure at high-impact velocities, crucial for their performance as energy absorbers. Plastic deformation observed during compression tests indicated the structures' ability to absorb energy, with cracked surfaces revealing deformation patterns [22].

The research paper by Syrlybayev *et al.* [23], focuses on the compressive behavior analysis of pillar octahedral lattice structures, which are renowned for their high strength-to-weight ratio. Additive manufacturing technologies have facilitated the fabrication of complex lattice structures, spurring increased interest in their mechanical properties. Syrlybayev *et al.* [23], specifically investigates lattice structures with varying strut diameters (1.5, 1.75, and 2 mm) made from Tough PLA) plastic. The results indicate that increasing the strut diameter enhances strength and elastic moduli, while specific mechanical properties remain relatively constant. Both experimental and numerical analyses by Syrlybayev *et al.* [23], reveal that lattice structures fail due to the formation of diagonal shear bands.

The quest for sustainable solutions necessitates the development of materials that can increase efficiency, minimize environmental impact, and withstand operational stress and strain. Lattice structures, with their distinct mechanical properties and design flexibility, present a promising alternative to solid materials. However, the practical deployment of these structures in sustainable energy applications requires extensive research into their manufacturing processes, material selection, and performance under a variety of conditions. Despite the overwhelming benefits of lattice structures and additive manufacturing, there is a need for comprehensive research into the suitability of different materials, such as PLA (as used in this report), as well as the impact of environmental factors, such as UV (Ultraviolet) radiation, on the long-term performance of the structures.

The aim of this work was to investigate the effects of UV-induced aging on the mechanical properties of 3D-printed PLA lattice structures. This study specifically focuses on understanding how prolonged exposure to UV radiation impacts the compressive strength, Young's modulus, displacement at maximum compression force, and compressive strain of PLA lattice structures. By systematically analyzing these properties over different aging durations, this research aimed to provide insights to inform the design and application of PLA materials in environments with significant UV exposure.

2. Methodology

The design of this lattice structure with focus on the capability for additive manufacturing was done using Siemens NX Software tool. These design that aimed at enhanced mechanical properties such as weight, stiffness, strength, impact resistance, deformation, durability, scalability and complex geometry with

specified dimension of 40mm cube and each workpiece having 8mm² perforation to attain 50.4% porosity as shown in figure 1 is geared towards optimum performance when subjected to test.

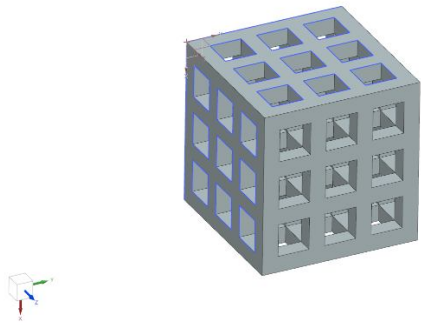


Figure 1. Desired 3D Lattice structure ready for printing

2.1. Printing of Lattice Structure

PLA filament with a lower melting point between 180^oc and 220^oc is used as a printed material for the development of the 3D lattice structure using additive manufacturing. The additive manufacturing process with the precise nozzle diameter and the specified layer height can generate a complex geometry and lattice configuration that would normally be challenging to manufacture with the use of traditional manufacturing process with large printed infills. For optimum printing, there is usually a preliminary test to calibrate the printer settings. Twelve (12) different sets of the lattice structure were printed with each weighing 39.93g with an approximation to 3 decimal places. The mass of the infills manually removed from each piece was about 13.72g as shown in figure 3 to give the desired output as shown in figure 2.

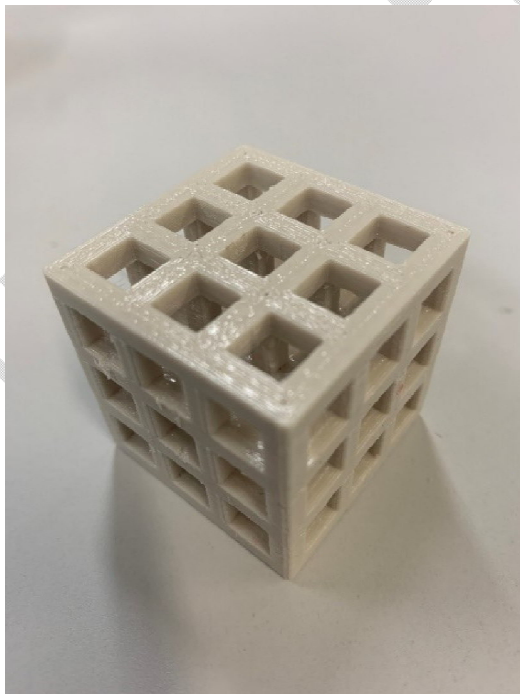


Figure 2. 3D printed copy of the lattice structure

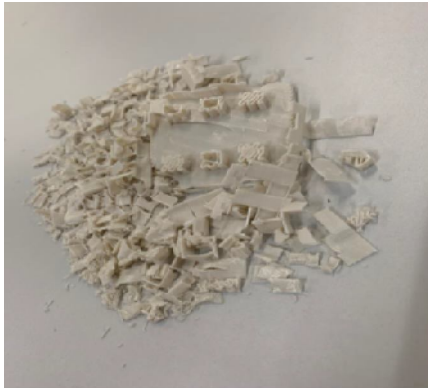


Figure 3. Manually removed Infills

2.2. Aging Test

The aging test was carried out to evaluate the lattice structures' performance over a period when simulated in different environmental conditions. This test determines the behavior and performance of the lattice structures. The BGD 852 Bench UV Light Accelerated Aging Test Chamber shown in figure 4 was used to subject the lattice structure to varying exposure under the high UV radiation to test the tolerance, resistance to degradation, color fading, brittleness and overall structural integrity over time by simulating years of exposure to sunshine in a fraction of days.

The UVA-340 lamps used in the accelerated weathering chamber have a wavelength range of 365 to 295 nm, which is remarkably similar to the short-wave ultraviolet radiation of solar spectrum.

Photodegradation is the alteration of a material caused by photons, particularly those present in the wavelengths of sunlight which offer about 0.7 W/m^2 of irradiance. Three sets of **three** pieces **of the specimens** were subjected to radiation of temperature 45°C and a relative humidity of 65% for a period of 4, 6 and 8 weeks. The resultant lattice structure is further taken to another compression test.



Figure 4. BGD 852 Bench UV Accelerated Cabinet with first sets of cubes under UV Light

2.3. Compression Test

To determine the mechanical strength and percentage deformation of the lattice structure, the 3367 Series Dual Tabletop Testing System is used to apply controlled compressive uniform force to the lattice structure as shown in figure 5. Lattice structure was placed centrally on the lower compression plate for uniform load distribution, the upper plate is set to gently contact the top of lattice structure, the machine is then set to compress at a constant rate **for all the specimens**, while the force and displacement data are monitored and recorded for analysis until maximum displacement is reached. The result can be used to plot the force displacement curve while the lattice structure is then removed and inspected for deformation features.

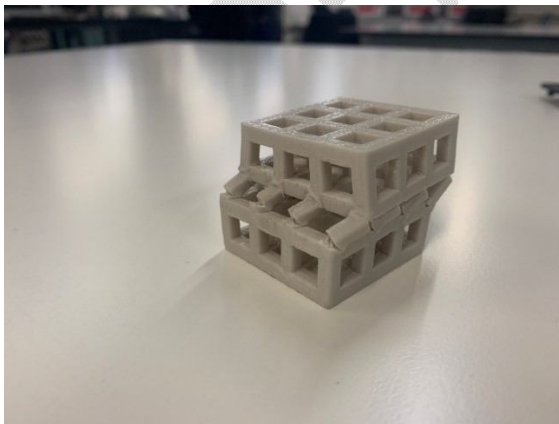


Figure 5. Deformation of a compressed 3D lattice structure

3. Result and Analysis

Table 1. Control compression test data

Prototype	Max Force (kN)	Compressive Strength (MPa)	Young's Modulus (Automatic) (MPa)	Displacement at Max Compressive Force (mm)	Compressive strain (Displacement) at Max Compressive Force (%)
A	15.72	9.82	212.21	2.40	6.00
B	15.06	9.41	118.07	2.27	5.67
C	17.53	10.95	283.71	3.50	8.75
Mean	16.10	10.06	204.66	2.72	6.81
Standard deviation	1.28	0.80	83.07	0.68	1.69
Mini	15.06	9.41	118.07	2.27	5.67
Max	17.53	10.95	283.71	3.50	8.75
Range	2.47	1.54	165.63	1.23	3.08

Graph 1

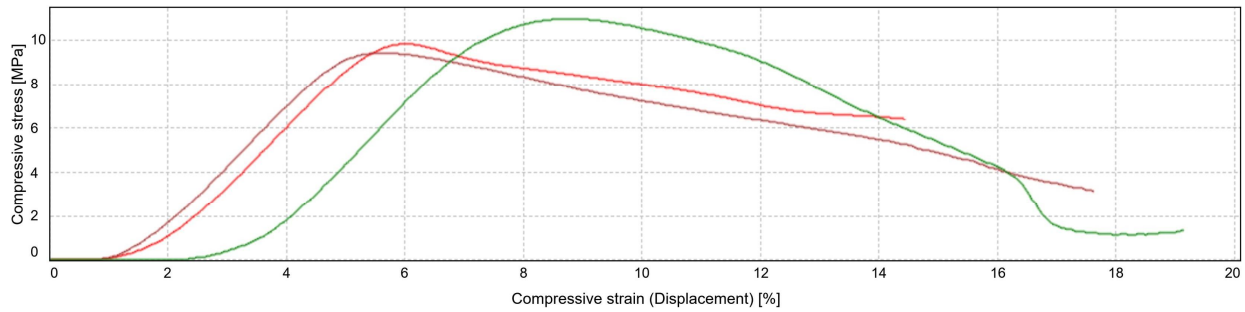


Figure 6. Control stress-displacement graph

Table 2. 4-week compression test data

Prototype	Max Force (kN)	Compressive Strength (MPa)	Young's Modulus (Automatic) (MPa)	Displacement at Max Compressive Force (mm)	Compressive strain (Displacement) at Max Compressive Force (%)
A	17.35	10.84	276.64	3.38	8.46

B	16.08	10.05	276.18	3.35	8.38
C	15.68	9.80	274.37	3.38	8.46
Mean	16.37	10.23	275.73	3.37	8.43
Standard deviation	0.87	0.54	1.20	0.02	0.05
Mini	15.68	9.80	274.37	3.35	8.38
Max	17.35	10.84	276.64	3.38	8.46
Range	1.66	1.04	2.27	0.03	0.08

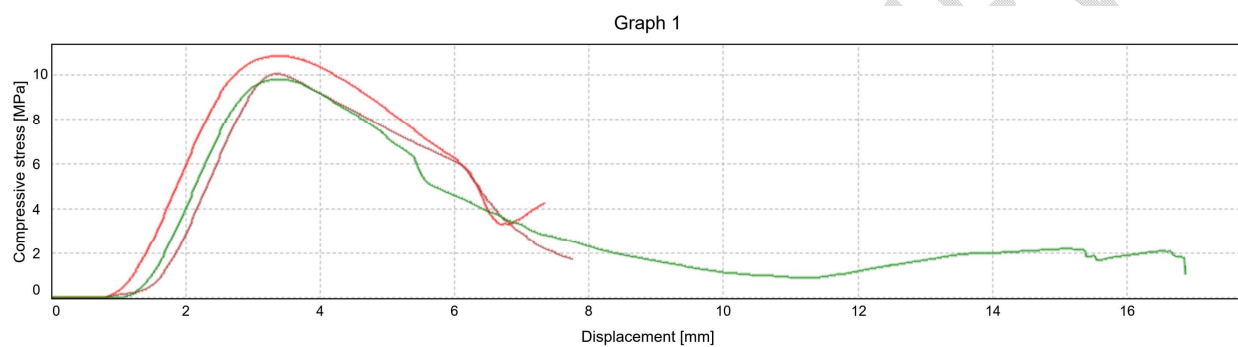


Figure 7. 4-week stress-displacement graph

Table 3. 6-week compression test data

Prototype	Max Force (kN)	Compressive Strength (MPa)	Young's Modulus (Automatic) (MPa)	Displacement at Max Compressive Force (mm)	Compressive strain (Displacement) at Max Compressive Force (%)
A	15.76	9.85	266.49	2.82	7.04
B	16.28	10.18	281.64	3.30	8.25
C	18.65	11.65	288.74	3.93	9.83
Mean	16.90	10.56	278.96	3.35	8.38
Standard deviation	1.54	0.96	11.37	0.56	1.40
Mini	15.76	9.85	266.49	2.82	7.04
Max	18.65	11.65	288.74	3.93	9.83
Range	2.89	1.81	22.25	1.12	2.79

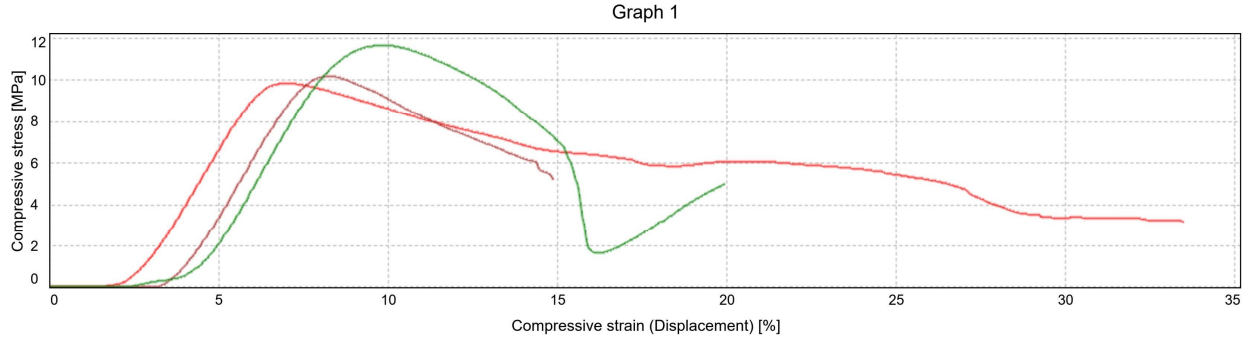


Figure 8. 6-week stress-displacement graph

Table 4. 8-week compression test data

Prototype	Maxi Force [kN]	Compressive Strength [MPa]	Young's Modulus (Automatic) [MPa]	Displacement at Max Compressive Force (mm)	Compressive strain (Displacement) at Max Compressive Force (%)
A	18.21	11.38	304.14	3.07	7.67
B	15.26	9.54	262.66	3.58	8.96
C	17.93	11.20	291.25	2.97	7.42
Mean	17.13	10.71	286.02	3.21	8.02
Standard deviation	1.63	1.02	21.23	0.33	0.83
Mini	15.26	9.54	262.66	2.97	7.42
Maxi	18.21	11.38	304.14	3.58	8.96
Range	2.95	1.84	41.48	0.62	1.54

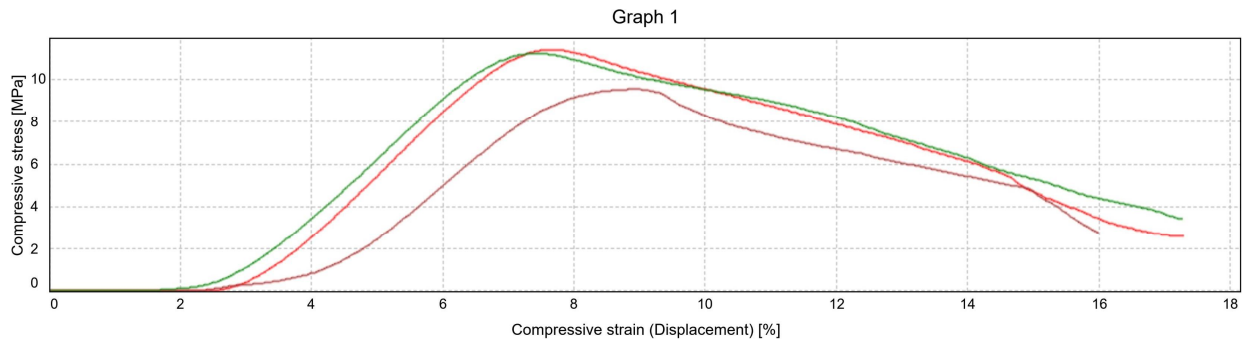


Figure 9. 8-week stress-displacement graph

In the foremost phases of compression, the stress-displacement curves for figure 6, figure 7, figure 8 and figure 9 exhibit a linear relationship, which shows indication of elastic deformation, and an extensive

analysis of the data leveraged by data visualization on Power BI (Business Intelligence) reveals the transformation in the PLA's mechanical properties.

The Young's modulus as shown in equation 1, a measure of a material's stiffness, is a critical parameter in understanding the mechanical properties of the PLA lattice structures.

$$\text{Young Modulus, } \gamma \text{ (N/m}^2\text{)} = \frac{\text{Compression Stress, } \sigma \text{ (N/m}^2\text{)}}{\text{Engineering Strain, } \epsilon} \quad (1)$$

From table 1, the control prototypes, which were not subjected to UV aging, had a mean Young's modulus of 204.66 MPa. This baseline value reflects the initial stiffness of the PLA lattice structures, indicating its ability to resist deformation under an applied load. For 4 weeks of accelerated UV exposure, the mean Young's modulus increased to 275.73 MPa as shown in table 2, which shows that the material became stiffer due to the UV aging process. The mean Young's modulus further increased to 278.96 MPa as shown in table 3 for 6 weeks of accelerated UV exposure. Although the rate of increase slowed compared to the initial 4 weeks, the continued rise in Young's modulus indicates ongoing changes in the material's internal structure, likely due to prolonged exposure to UV radiation. For 8 weeks of accelerated UV exposure, the mean Young's modulus reached 286.02 MPa as shown in table 4. This continued increase confirms that prolonged UV exposure progressively makes the PLA lattice structures more brittle and stiffer. The trend as shown in figure 10 suggests a significant alteration in the material properties, which can be attributed to the cumulative effects of UV-induced degradation, as UV radiation typically leads to the photo-degradation of polymers, causing chain scission and cross-linking, which can result in increased brittleness and stiffness. This behavior is typical of polymer degradation, where UV radiation causes changes in the molecular structure, leading to increased rigidity.

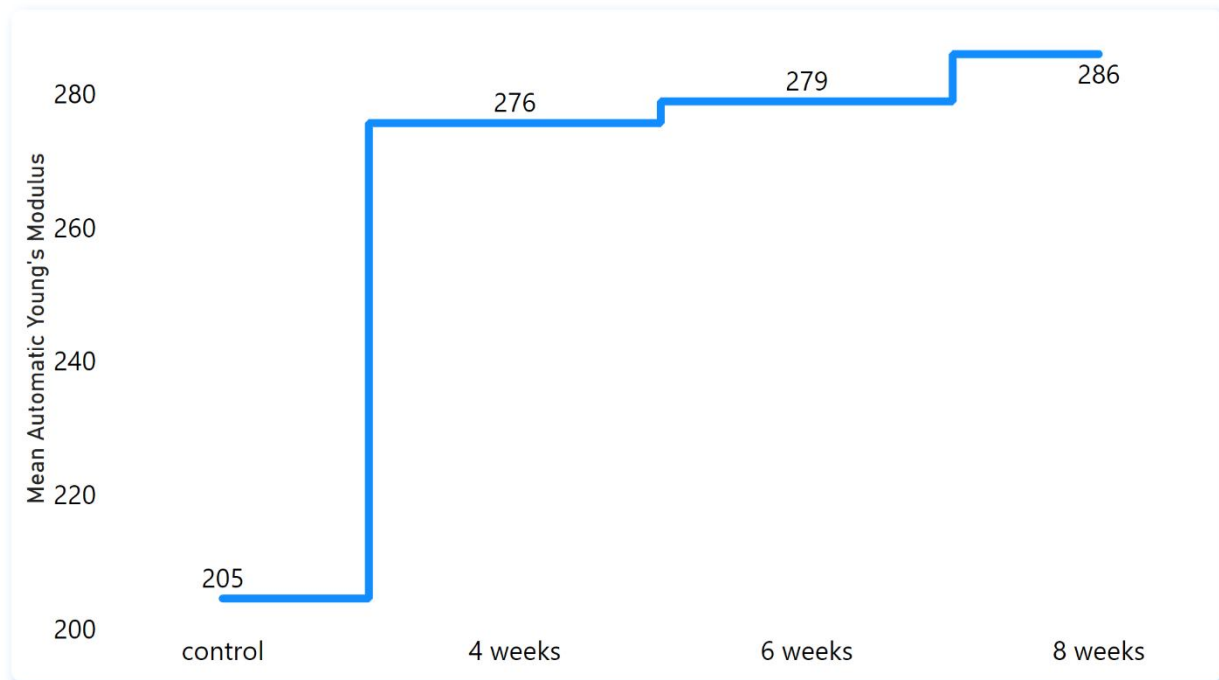


Figure 10. Mean Young's modulus

The compressive strength of a material as shown in equation 2, which measures the ability of the material to withstand compressive loads, is a crucial property for evaluating the mechanical performance of PLA lattice structure.

$$\text{Compression Stress, } \sigma \text{ (N/m}^2\text{)} = \frac{\text{Force, } f \text{ (N)}}{\text{Area, } A \text{ (m}^2\text{)}} \quad (2)$$

Analysis of the compressive strength from control prototypes to those subjected to the accelerated UV exposure for 4, 6, and 8 weeks provides insights into the material's behavior under prolonged environmental stress. From table 1, the control prototypes, which were not subjected to the accelerated UV aging, exhibited a mean compressive strength of 10.06 MPa, which represents the baseline value of the initial load-bearing capacity of the PLA lattice structure before any degradation. For 4 weeks of accelerated UV exposure, the mean compressive strength increased slightly to 10.23 MPa as shown in table 2. This modest increase suggests that the initial stages of the accelerated UV aging might have led to some degree of hardening or embrittlement, which could enhance the material's ability to bear compressive loads in the short term. From table 3, the mean compressive strength further increased to 10.56 MPa for 6 weeks of accelerated UV exposure. This continued rise indicates that the material's internal structure changed due to prolonged UV exposure, which led to additional hardening effects. For 8 weeks of accelerated UV exposure, the mean compressive strength reached 10.71 MPa as shown in table 4. This trend of increasing compressive strength with extended accelerated UV exposure as shown in figure 11 suggests that the material continues to undergo changes that enhance its load-bearing capacity. However, it's important to note that this increased strength is due to its increased brittleness, as indicated by accompanying Young's modulus.

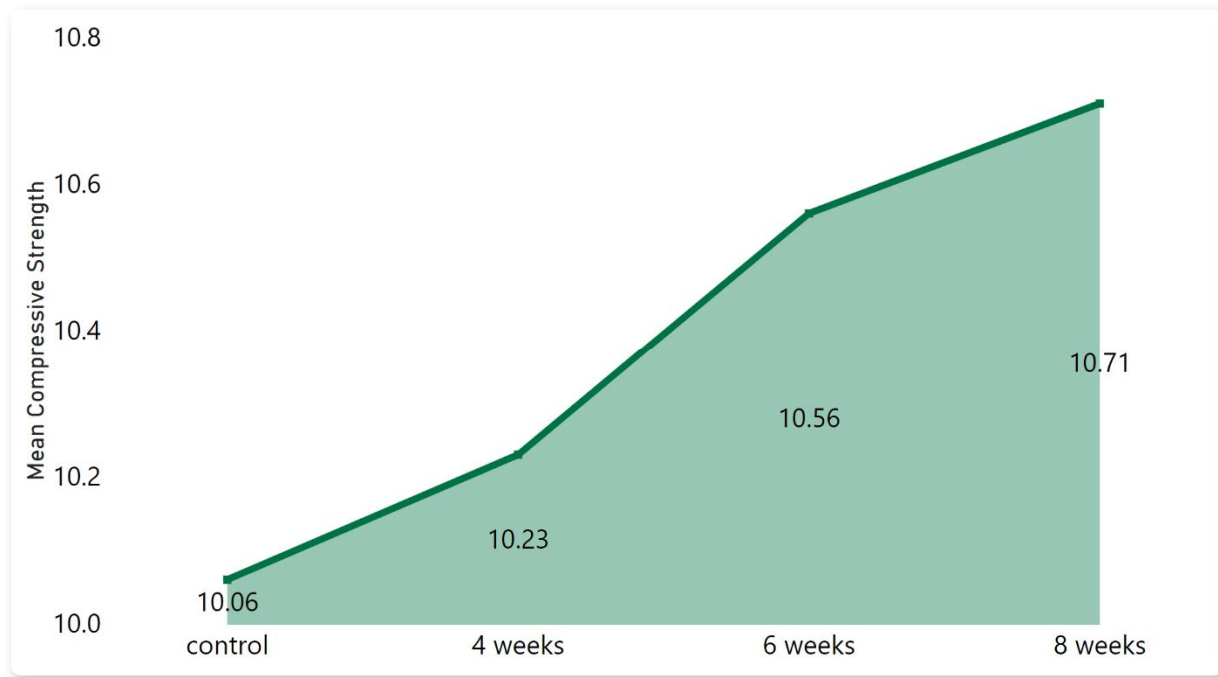


Figure 11. Mean compressive strength

Displacement at maximum compression force is a crucial parameter for understanding how much a material deforms under its maximum load bearing capacity. The control prototypes, which were not subjected to UV aging, exhibited a mean displacement at maximum compression force of 2.72 mm as shown in table 1, which reflects the initial deformability of the PLA lattice structures under peak load conditions. For 4 weeks of accelerated UV exposure, the mean displacement at maximum compression force increased to 3.38 mm as shown in table 2. This increase indicates that the material becomes more deformable with initial UV exposure, suggesting changes in the internal structure that reduce the material's resistance to deformation under load. From table 3, the mean displacement further increased to 3.93 mm for 6 weeks of accelerated UV exposure. This continued rise in displacement suggests that the material is undergoing significant structural changes, likely due to the prolonged effects of UV radiation. For 8 weeks of accelerated UV exposure, the mean displacement at maximum compression force decreased to 3.21 mm as shown in table 4. This decrease may indicate a complex interaction of factors affecting the material's behavior. While the material continues to degrade, increased cross-linking or other structural changes might be contributing to a reduction in displacement. Figure 12 shows the overall trend of increased deformability with accelerated UV exposure, which highlights the potential risks to structural integrity and load-bearing capacity over time.

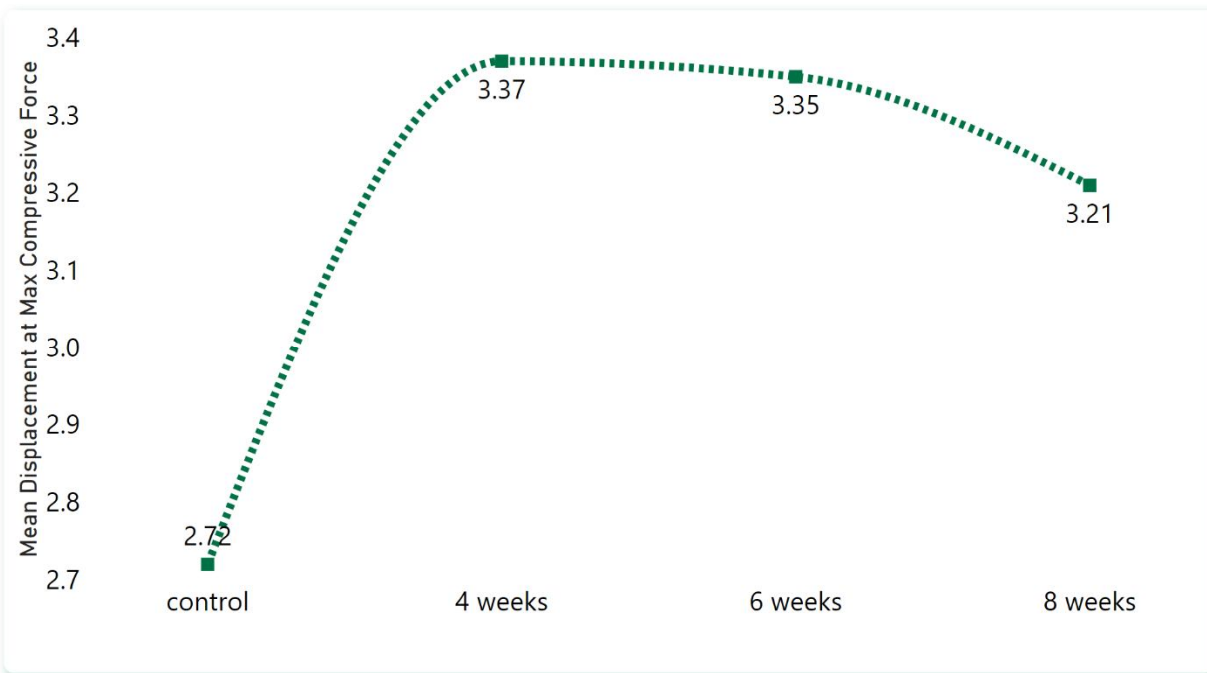


Figure 12. Mean displacement at maximum compression force

Compressive strain at maximum compression force is a measure of the deformation of a material relative to its original dimensions when subjected to its maximum load-bearing capacity. The control prototypes, which were not subjected to UV aging, exhibited a mean compressive strain at maximum compression force of approximately 6.8% as shown in table 1. This baseline value indicates the initial deformation capability of the PLA lattice structures under maximum load. For 4 weeks of accelerated UV exposure, the mean compressive strain at maximum compression force increased to approximately 8.5% as shown in table 2. This increase suggests that the material becomes more deformable with initial UV exposure, indicating structural changes that reduce the material's resistance to deformation. From table 3, the mean

compressive strain further increased to approximately 9.8% for 6 weeks of accelerated UV exposure. This continued rise in compressive strain indicates significant structural changes within the PLA lattice structures due to prolonged UV exposure, leading to increased deformability. For 8 weeks of accelerated UV exposure, the mean compressive strain at maximum compression force decreased to approximately 8.0% as shown in table 4. This decrease suggests a complex interaction of degradation processes. Figure 13 shows the overall trend of increased compressive strain with accelerated UV exposure, which highlights the potential risks to the mechanical performance and durability of the PLA lattice structures, indicating that the PLA lattice structures become progressively more deformable under maximum compression force with accelerated UV exposure.

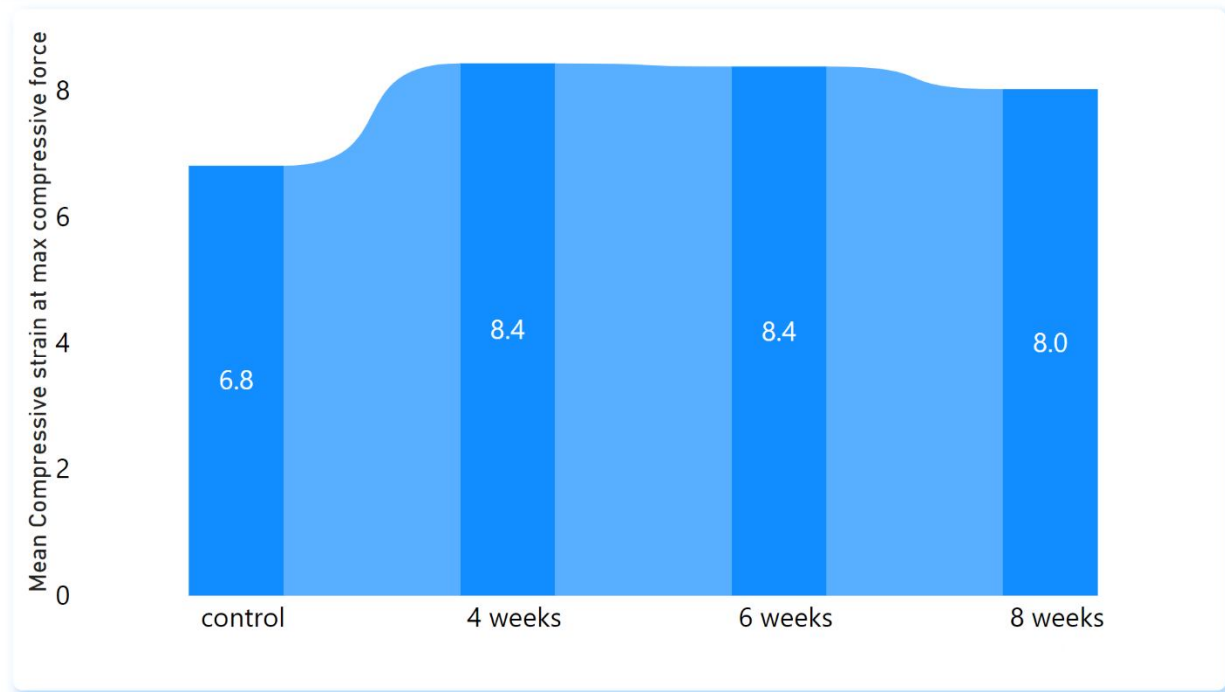


Figure 13. Mean compressive strain at maximum compression force

UV radiation can induce cross-linking in the polymer chains of PLA, which increases the stiffness of the material, and cross-linking creates a network of bonds that restricts the mobility of polymer chains, leading to an increase in Young's modulus. Simultaneously, UV radiation can cause chain scission, breaking down long polymer chains into shorter segments, while chain scission generally leads to material degradation, in the initial stages, the resultant cross-linking can dominate, thereby increasing stiffness. The combined effects of cross-linking and chain scission make the material more brittle, as indicated by the increase in Young's modulus, this embrittlement is a common response of polymers to UV exposure.

The cross-linking induced by UV radiation not only increases stiffness but also enhances the load-bearing capacity of the material and the formation of a more tightly bonded network which improves the material's ability to resist compressive forces. UV exposure can lead to changes in the microstructure of PLA, such as increased crystallinity, and a higher crystallinity can contribute to improved compressive strength as crystalline regions are generally stronger and stiffer than amorphous regions. UV exposure can also cause surface hardening, leading to an increase in compressive strength, and the hardened surface can better distribute and resist applied loads.

The increase in compressive strain suggests that the material, while becoming more brittle, also exhibits increased plastic deformation under compressive loads, which is likely due to the initial breakdown of the polymer matrix, making the material more deformable before it ultimately fails. UV radiation primarily affects the amorphous regions of PLA, leading to greater mobility and deformability in these regions, and the increased compressive strain indicates that the material can endure more deformation relative to its original dimensions before failure. Prolonged UV exposure can lead to the formation of micro-cracks and stress concentrations within the material, and these defects allow for more significant deformation under load, indicating progressive deterioration in the material.

The increased stiffness and brittleness suggest that while the PLA's ability to bear compressive loads may improve slightly, its overall durability and resilience to impact or dynamic loading conditions may be compromised, because brittle materials are more prone to cracking and failure under stress, which is an important consideration for long-term applications. Understanding these changes are crucial for applications where PLA lattice structures are exposed to environmental conditions, and Engineers must account for the potential increase in brittleness and adjust their designs accordingly to ensure long-term reliability and performance.

When designing components for environments with significant UV exposure, engineers must consider the trade-offs between increased stiffness and brittleness. Understanding the changes in its mechanical properties helps predict the long-term performance of PLA structures, and this knowledge is crucial for ensuring the reliability and safety of components over their expected lifespan. The insights from this study can guide application-specific adjustments, such as optimizing lattice geometries or combining it with other materials to balance stiffness and deformability or selecting appropriate manufacturing processes to enhance structural performance. Saleh *et al.* [18] in their study used Carbon Fiber-PLA, and it demonstrated a substantial increase in the Young's modulus due to the reinforcing effect of carbon fibers, enhancing stiffness without the adverse effects of brittleness, as the fibers provide a direct reinforcement, resulting in a more substantial and controlled improvement in load-bearing capacity, for an enhanced resistance to deformation.

Conclusion

The study successfully demonstrated the design, manufacturing, and testing of PLA lattice structures, providing valuable insights into their mechanical properties and performance under various conditions. The accelerated aging tests, simulating UV radiation exposure, revealed significant changes in the mechanical properties of the PLA prototypes. As the exposure duration increased, the material exhibited increased brittleness, higher Young's modulus, and enhanced compressive strength, indicating an improved resistance to compression at the expense of flexibility. The compression tests further validated these findings, showing that prolonged UV exposure leads to increased displacement and compressive strain at maximum compression force, highlighting the material's progressive deterioration and increased deformability over time.

These results provide critical insights into the aging behavior of PLA, demonstrating that environmental factors such as UV radiation significantly impact its mechanical properties. The research underscores the importance of considering these factors in material selection and design for applications requiring long-term durability. The findings will guide future design iterations, material selection strategies, and engineering decisions, contributing to the development of more resilient and efficient lattice structures.

Overall, this study highlights the effectiveness of combining advanced design software, additive manufacturing, and rigorous testing methodologies to innovate and optimize material performance in real-world applications. The knowledge gained from this research will be instrumental in advancing the field of material science and engineering, particularly in the context of sustainable and high-performance lattice structures.

Recommendations for Further Work

Studies can be conducted with extended accelerated UV exposure times beyond 8 weeks, so as to observe the longer term effects on its mechanical properties, and diverse environmental conditions can be explored, so as to observe the effects of other environmental factors such as varying humidity levels and temperature fluctuations based on the seasons of the year.

Disclaimer (Artificial intelligence)

Option 1:

Author(s) hereby declare that NO generative AI technologies such as Large Language Models (ChatGPT, COPILOT, etc) and text-to-image generators have been used during writing or editing of manuscripts.

Option 2:

Author(s) hereby declare that generative AI technologies such as Large Language Models, etc have been used during writing or editing of manuscripts. This explanation will include list the name, version, model, and source of the generative AI technology and as well as the all input prompts provided to a generative AI technology

Details of the AI usage are given below:

- 1.
- 2.
- 3.

References

1. Nagesha BK, Dhinakaran V, Varsha Shree M, Manoj Kumar KP, Chalawadi D, Sathish T. Review on characterization and impacts of the lattice structure in additive manufacturing. *Materials Today: Proceedings*. 2020;21(1):916–9. <https://doi.org/10.1016/j.matpr.2019.08.158>
2. Ataollahi S. A review on additive manufacturing of lattice structures in tissue engineering. *Bioprinting*. 2023;35:e00304. <https://doi.org/10.1016/j.bprint.2023.e00304>
3. Tao W, Leu MC. Design of lattice structure for additive manufacturing. *IEEE Xplore*. 2016;325–32. <https://doi.org/10.1109/isfa.2016.7790182>
4. Chen LY, Liang SX, Liu Y, Zhang LC. Additive manufacturing of metallic lattice structures: Unconstrained design, accurate fabrication, fascinated performances, and challenges. *Materials Science and Engineering: R: Reports*. 2021;146:100648. <https://doi.org/10.1016/j.mser.2021.100648>

5. Muthe LP, Pickering K, Gauss C. A Review of 3D/4D Printing of Poly-Lactic Acid Composites with Bio-Derived Reinforcements. *Composites Part C: Open Access*. 2022;8:100271. <https://doi.org/10.1016/j.jcomc.2022.100271>
6. Gauss C, Pickering KL, Graupner N, Müssig J. 3D-printed polylactide composites reinforced with short lyocell fibres – Enhanced mechanical properties based on bio-inspired fibre fibrillation and post-print annealing. *Additive Manufacturing*. 2023;77:103806. <https://doi.org/10.1016/j.addma.2023.103806>
7. Mastalygina EE, Aleksanyan KV. Recent Approaches to the Plasticization of Poly(lactic Acid) (PLA) (A Review). *Polymers*. 2024;16(1):87. <https://doi.org/10.3390/polym16010087>
8. Cristina K, Shayene A, Jacobus H. Cellulose-Reinforced Polylactic Acid Composites for Three-Dimensional Printing Using Polyethylene Glycol as an Additive: A Comprehensive Review. *Polymers*. 2023;15(19):3960–0. <https://doi.org/10.3390/polym15193960>
9. Maconachie T, Leary M, Lozanovski B, Zhang X, Qian M, Faruque O, et al. SLM lattice structures: Properties, performance, applications and challenges. *Materials & Design [Internet]*. 2019 Dec;183:108137. <https://doi.org/10.1016/j.matdes.2019.108137>
10. Mahmoud D, Elbestawi M. Lattice Structures and Functionally Graded Materials Applications in Additive Manufacturing of Orthopedic Implants: A Review. *Journal of Manufacturing and Materials Processing*. 2017;1(2):13. <https://doi.org/10.3390/jmmp1020013>.
11. Dong G, Tang Y, Li D, Zhao YF. Design and optimization of solid lattice hybrid structures fabricated by additive manufacturing. *Additive Manufacturing*. 2020;33:101116. <https://doi.org/10.1016/j.addma.2020.101116>
12. Cuevas-Suárez CE, Meereis CTW, D'accorso N, Macchi R, Ancona-Meza AL, Zamarripa-Calderón E. Effect of radiant exposure and UV accelerated aging on physico-chemical and mechanical properties of composite resins. *Journal of Applied Oral Science*. 2019;27. <https://doi.org/10.1590/1678-7757-2018-0075>.
13. Andreia Araújo, Gabriela Lema Botelho, Manuela Silva, Ana Vera Machado. UV Stability of Poly(Lactic Acid) Nanocomposites. *Journal of Materials Science and Engineering B*. 2013;3(2). <https://doi.org/10.17265/2161-6221/2013.02.001>.
14. Rasselet D, Ruellan A, Guinault A, Miquelard-Garnier G, Sollogoub C, Fayolle B. Oxidative degradation of polylactide (PLA) and its effects on physical and mechanical properties. *European Polymer Journal*. 2014;50:109–16. <https://doi.org/10.1016/j.eurpolymj.2013.10.011>
15. Hardy C, Kociok-Köhn G, Buchard A. UV degradation of poly(lactic acid) materials through copolymerisation with a sugar-derived cyclic xanthate. *Chemical Communications*. 2022;58(36):5463–6. <https://doi.org/10.1039/d2cc01322c>.
16. Aleksandra Kalwik, Przemyslaw Postawa, Marcin Nabialek. Analysis of Ageing Processes of Semi-Crystalline Materials. *Materialeplastiche*. 2020;57(3):41–51. <https://doi.org/10.37358/mp.20.3.5378>.
17. Wang J, Gu Z, Zhao J, Zhang S, Li P, Meng C, et al. Aging behavior of three-proof polyurethane coatings under UV radiation. *Polimery*. 2022;67(9):433–7. <https://doi.org/10.14314/polimery.2022.9.4>.
18. Saleh M, Anwar S, Abdulrahman Al-Ahmari, Abdullah Alfaify. Compression Performance and Failure Analysis of 3D-Printed Carbon Fiber/PLA Composite TPMS Lattice Structures. *Polymers*. 2022;14(21):4595–5. <https://doi.org/10.3390/polym14214595>.
19. Du C, Li H, Yan S, Zhang Q, Jia J, Chen X. Damage and failure analysis of composite stiffened panels under low-velocity impact and compression after impact with damp-heat aging. *Science and Engineering of Composite Materials*. 2022;29(1):378–93. <https://doi.org/10.1515/secm-2022-0159>.

20.Nichita-Larisa Milodin, Popa NM, Mihai Tutoveanu, Flavia-Petruta-Georgiana Artimon. Compression Testing of PA2200 Additive Manufactured Lattice Structures. International Conference on Reliable Systems Engineering (ICoRSE). Lecture Notes in Networks and Systems, Jul 28.2021;305:304–15.https://doi.org/10.1007/978-3-030-83368-8_30.

21.Jeon MH, Cho HJ, Lee MY, Kim YJ, Kim IG. Compressive strength prediction of composite lattice structure using compression test results of sub element specimens. Mechanics of advanced materials and structures. 2023;Mar 30;1–15.<https://doi.org/10.1080/15376494.2023.2175082>.

22.Akbay ÖC, Özdemir B, Bahçe E, Emir E. Deformation Behaviors Investigation of CoCr Alloy Lattice Structures under Compression Test. Journal of Manufacturing Engineering. 2023;18(1):001-010.<https://doi.org/10.37255/jme.v18i1pp001-010>.

23.Daniyar Syrlybayev, Perveen A, Didier Talamona. Compression Behavior of Pilar Octahedral Lattice Structures. Materials science forum. 2023;1087:143–8.<https://doi.org/10.4028/p-8p61q8>.

UNDER PEER REVIEW